

Low-energy kink in the nodal dispersion of copper-oxide superconductors: Insights from Dynamical Mean Field Theory

Johannes Bauer¹ and Giorgio Sangiovanni²

¹*Max-Planck Institute for Solid State Research, Heisenbergstr.1, 70569 Stuttgart, Germany and*

²*Institute of Solid State Physics, Vienna University of Technology, 1040 Vienna, Austria*

(Dated: February 23, 2024)

Motivated by the observation in copper-oxide high-temperature superconductors, we investigate the appearance of kinks in the electronic dispersion due to coupling to phonons for a system with strong electronic repulsion. We study a Hubbard model supplemented by an electron-phonon coupling of Holstein type within Dynamical Mean Field Theory (DMFT) utilizing Numerical Renormalization Group as impurity solver. Paramagnetic DMFT solutions in the presence of large repulsion show a kink only for large values of the electron-phonon coupling λ or large doping and, contrary to the conventional electron-phonon theory, the position of such a kink can be shifted to energies larger than the renormalized phonon frequency ω_0^r . When including antiferromagnetic correlations we find a stronger effect of the electron-phonon interaction on the electronic dispersion due to a cooperative effect and a visible kink at ω_0^r , even for smaller λ . Our results provide a scenario of a kink position increasing with doping, which can be related to recent photoemission experiments on Bi-based cuprates.

PACS numbers: 74.72.-h, 71.38.Mx, 71.10.Fd, 71.20.Tx, 71.10.-w, 63.20.Kr

I. INTRODUCTION

One of the manifestations of a strong coupling between condensed matter electrons and lattice vibrations is the occurrence of kinks (abrupt changes of the slope) in the electronic dispersion relation. Such kinks occur at a certain energy associated with a phonon mode and their strength is directly related to the electron-phonon coupling constant λ . Therefore the observation of a kink, for instance, in angle resolved photoemission (ARPES) data, is often taken as an indication that a system possesses a strong electron-phonon coupling and its properties are likely to be strongly influenced by this. However, also coupling to other bosonic modes possibly of purely electronic origin, can have the same effect on the dispersion relation. Moreover, in addition to an electron-phonon coupling different interactions important at low energy can compete or cooperate with it, which may modify the picture. Therefore, the experimental observation must be analyzed carefully before conclusions about the origin of a kink can be made.

Prominent examples for the observation of kinks come from the field of cuprate superconductors. Studies by Lanzara *et al.*¹ collected evidence for this in different compounds. One interpretation of these experiments is that the dispersion kink along the nodal direction of the Brillouin zone is associated to a longitudinal in-plane bond-stretching mode in which two of the four oxygen atoms surrounding the copper move inwards (“half-breathing” mode)². The same phonon mode indeed displays a sizable renormalization in inelastic neutron scattering measurements³, pointing towards a strong coupling to carriers. This conclusion is further supported by Iwasawa *et al.*⁴, who carefully studied the effect of an ¹⁶O-¹⁸O isotope substitution and concluded that their observation is compatible with the “half-breathing”

mode. On the other hand, recent work by Dahm *et al.*⁵ emphasized the connection between the nodal kink and spin-fluctuations, an alternative scenario.^{6–9} Hence, presently no general consensus exists on this important issue of high-temperature superconductors.¹⁰ A review article covering numerous aspects of this topic has been recently published by A. S. Mishchenko¹¹.

One of the aspects of the nodal kink which is particularly puzzling is the doping dependence of its position. Early studies indicated that the nodal kink occurs at a more or less constant energy position¹². A more recent study by Kordyuk *et al.*¹³ showed however that in LSCO the kink position ω_k first increases with doping, exhibits a maximum around optimal doping, and eventually decreases again, in a dome-like shape. In Bi-2212 the situation is even more intricate as the non-monotonic dependence is replaced, at low temperatures, by a peculiar increase upon increasing doping. Such a pronounced doping and temperature dependence is a very strong indication that the nodal kink in cuprates cannot be described within the textbook picture of conventional metals with electron-phonon interaction.

The standard description of effects of electron-phonon coupling is based on perturbation theory in the electron-phonon coupling constant assuming that electrons can be described as a weakly interacting Fermi liquid¹⁴. Then, to lowest order in the coupling the magnitude of a kink, m_k , in the electronic dispersion relates to the dimensionless electron-phonon coupling λ as $m_k = 1 + \lambda$. A clear kink, however, points to a relatively strong electron-phonon coupling, for which one expects effects beyond the lowest order diagrams and possibly vertex corrections to become very important. Vertex corrections are beyond the Migdal-Eliashberg formalism, i.e. beyond the most common diagrammatic theory for the electron-phonon interaction.^{15–17}. If on top of that one takes also the

electron-electron interaction and Mott physics into account, as in any minimal model for high-temperature cuprate superconductors, a quantitative description of the nodal kink within conventional theories seems inconceivable.

Substantial progress in understanding strongly coupled electron-phonon systems has been developed in recent years based on dynamical mean field (DMFT) methods¹⁸ and cluster extensions¹⁹. The advantage of these approaches is that electron-electron and electron-phonon interactions are treated non-perturbatively and on equal footing^{20–27}. One major insight of these studies is that the electron-phonon interaction in strongly correlated metals cannot be understood with conventional tools. In particular, the polaronic signatures in photoemission spectra are more complicated than what suggested by perturbation theory on top of a Fermi liquid solution¹⁴. This is also in line with the conclusions of other studies which do not rely on the dynamical mean field approximation^{28–30}.

Even though DMFT misses a crucial part of the non-local physics of the two-dimensional copper-oxygen planes, it is interesting to see whether some aspects of the nodal kink puzzle posed by recent experiments can be understood already within the purely local picture of the interplay between the electron-electron repulsion and the retarded phonon-mediated attraction given by DMFT. This is the motivation for the present study, which focuses on a description of the kinks in the electronic dispersion due to phonons in the presence of strong electronic correlations. We employ the numerical renormalization group (NRG)^{31,32} as DMFT impurity solver. NRG is known to have a good low energy resolution at low temperatures^{32–34}, and one can calculate spectral functions directly on the real axis, which makes it the method of choice for the analysis of low-energy kinks.

We first analyze paramagnetic (PM) solutions in the vicinity of half-filling and zero temperature. In order to see the effect of antiferromagnetic (AF) correlations, which are expected to be important in the cuprates, we also perform calculations in the commensurate AF state. The latter have been shown to successfully mimic the effect of antiferromagnetic correlations and exchange coupling J .^{35–37} Away from half filling the Hubbard model can show phase separation or incommensurate order, hence, the analysis of the results must be done very carefully.

Our study is based on a model Hamiltonian, Hubbard Holstein model, of the form

$$H = - \sum_{i,j,\sigma} (t_{ij} c_{i,\sigma}^\dagger c_{j,\sigma} + \text{h.c.}) + U \sum_i \hat{n}_{i,\uparrow} \hat{n}_{i,\downarrow} \quad (1)$$

$$+ \omega_0 \sum_i b_i^\dagger b_i + g \sum_i (b_i + b_i^\dagger) \left(\sum_\sigma \hat{n}_{i,\sigma} - 1 \right).$$

$c_{i,\sigma}^\dagger$ creates an electron at lattice site i with spin σ , and b_i^\dagger a phonon with oscillator frequency ω_0 , $\hat{n}_{i,\sigma} = c_{i,\sigma}^\dagger c_{i,\sigma}$. We include nearest neighbor hopping t_{ij} with magnitude t .

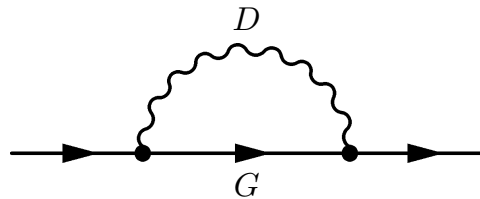


FIG. 1: Lowest order diagram for the electronic self-energy due to electron phonon coupling.

The electrons interact locally with strength U , and their density is coupled to a local phonon mode with coupling constant g . We have set the ionic mass to $M = 1$ in Eq. (1). We define $\lambda = \rho_0 2g^2 / \omega_0$ in terms of bare parameters where ρ_0 is the electronic density of states at the Fermi energy.

For the non-interacting density of states $\rho_0(\varepsilon)$ we take the semi-elliptic form $\rho_0(\varepsilon) = 2\sqrt{D^2 - \varepsilon^2} / (\pi D)^2$. In all the results we present here we take the value $W = 2D = 4t = 4$ for the bandwidth. The DMFT and NRG calculations are carried out as described in detail in Refs. 20,26,27,35,36.

The Paper is organized as follows: In section II we discuss the occurrence of kinks in the electronic dispersion in the normal, paramagnetic state. We first look at results for $U = 0$ and then analyze the situation for large U . In section III we show results when the effect of antiferromagnetic correlations are included in the calculations. In Section IV we conclude and relate our results to the experimental observations.

II. KINKS IN THE NORMAL STATE

Before analyzing the strong coupling situation we briefly recall the description of electron-phonon kinks in the weak coupling theory (for a review see, e.g., Refs. 38,39). In the paramagnetic state the Green's function reads,

$$G_{\mathbf{k}}(\omega) = \frac{1}{\omega - \varepsilon_{\mathbf{k}} + \mu - \Sigma(\omega)}, \quad (2)$$

where we assume a \mathbf{k} -independent self-energy.⁴⁰ Generally, the self-energy has contributions due to electron-phonon coupling g and electron-electron repulsion. The electron spectral function is given by $\rho_{\mathbf{k}}(\omega) = -\text{Im}G_{\mathbf{k}}(\omega)/\pi$ and the full (interacting) dispersion relation $E_{\mathbf{k}} = E(\varepsilon_{\mathbf{k}})$ by the maxima of $\rho_{\mathbf{k}}(\omega)$. This corresponds usually to the poles of Eq. (2), i.e. the solution of

$$E_{\mathbf{k}} - \varepsilon_{\mathbf{k}} + \mu - \text{Re}\Sigma(E_{\mathbf{k}}) = 0. \quad (3)$$

We define a kink as (more or less) abrupt change in the slope of $E(\varepsilon_{\mathbf{k}})$, which consequently must be found in $\text{Re}\Sigma(\omega)$.

In a calculation to order g^2 (depicted in Fig. 1) one finds that the $\text{Re}\Sigma(\omega)$ is roughly linear for small $|\omega| \ll \omega_0$,

$\text{Re}\Sigma^g(\omega) = -\lambda\omega$, strongly peaked at $\omega \simeq \omega_0$ (logarithmic divergence), and small for $|\omega| \gg \omega_0$. This yields for the low energy dispersion $E_{\mathbf{k}}^l = \varepsilon_{\mathbf{k}}/(1+\lambda)$ for $|E_{\mathbf{k}}| \ll \omega_0$ and $E_{\mathbf{k}}^h = \varepsilon_{\mathbf{k}}$ for $|E_{\mathbf{k}}| \gg \omega_0$. The magnitude of the kink is characterized by the ratio of the high energy over low energy slope, which gives $m_k = 1 + \lambda$ as mentioned earlier. This quantity is equal to the inverse of the quasiparticle renormalization factor Z and for a \mathbf{k} -independent self-energy to the effective mass $m^*/m_0 = Z^{-1}$. The free phonon propagator is sharply peaked at $|\omega| = \omega_0$. Due to the coupling to the electrons the peak can be shifted to a renormalized value ω_0^r and broadened. For the phonon properties, we consider the function $B(\omega) = \langle\langle b; b^\dagger \rangle\rangle_\omega$, which can be calculated in the NRG from the matrix elements and excitations. The corresponding spectral function is $\rho_b(\omega) = -\text{Im}B(\omega)/\pi$.

A. Results at $U = 0$

We first want to compare our DMFT-NRG results with the simple minded theory and consider the case $U = 0$. We use $\omega_0 = 0.2t$, and a filling factor of $n = 0.9$. In Fig. 2 (a) an example of the $\varepsilon_{\mathbf{k}}$ resolved spectral function $\rho_{\mathbf{k}}(\omega)$ is plotted for $\lambda = 0.29$.

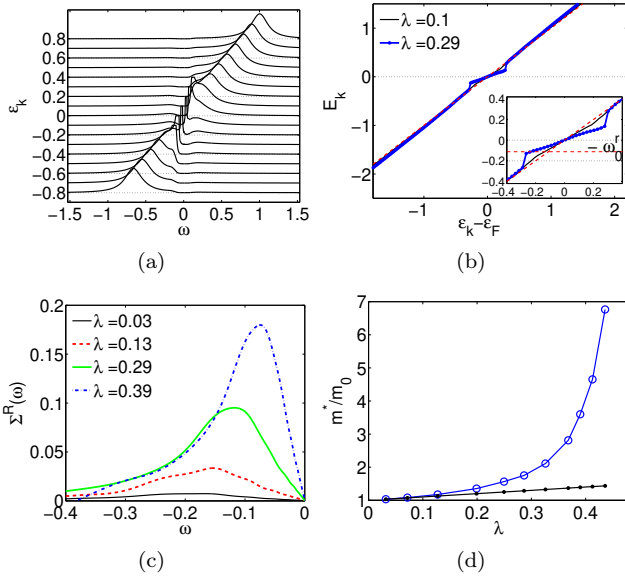


FIG. 2: (Color online) PM calculation: (a) The $\varepsilon_{\mathbf{k}}$ resolved spectral function for $U = 0$ and $\lambda = 0.29$. (b) The dispersion relation $E_{\mathbf{k}}$ as a function of $\varepsilon_{\mathbf{k}}$ for $U = 0$ and different values of electron-phonon coupling. The dashed line is for free electrons, $E_{\mathbf{k}} = \varepsilon_{\mathbf{k}}$. (c) The real part of the self-energy $\Sigma^R(\omega)$ (with $\Sigma^R(0)$ subtracted) as a function of ω for $U = 0$ and various values of λ . (d) The DMFT result for the effective mass (circles) compared with the second order perturbation theory result $1+\lambda$ (straight line).

We can see sharp quasiparticle peaks at low energy and broad peaks from certain energy on, $\omega_k \simeq \omega_0^r$, where the

kinks in the dispersion occurs (see Fig. 2 (b)). At this energy the imaginary part of the electronic self-energy sets in, and consequently the electronic spectrum becomes much broader.

The dispersion relation $E_{\mathbf{k}}$ is obtained numerically from the peak of position of $\rho_{\mathbf{k}}(\omega)$ as a function of $\varepsilon_{\mathbf{k}}$. It is shown for two values of λ in Fig. 2 (b). We find the picture of a kink as inferred from the lowest order g^2 diagram, i.e., the low energy dispersion is renormalized and at the (renormalized) phonon scale ω_0^r it reverts back to the non-interaction slope. The magnitude of the kink m_k can be inferred from the low-energy slope. For $\lambda = 0.29$, we find the value $m_k = 1.75$, whilst the corresponding value from the second order theory is with $m_k = 1.29$ substantially smaller. Comparing with part (a), we can also see how the discontinuity in the dispersion relation comes about through the change in maximum position.

The corresponding behavior of the real part of the self-energy, $\Sigma^R(\omega)$, is shown in Fig. 2 (c). We can see how the low energy slope increases with λ together with a peak at the renormalized phonon frequency ω_0^r , smaller than the bare value $\omega_0 = 0.2$. The renormalized phonon frequency ω_0^r as a function of λ is shown explicitly in Fig. 3.

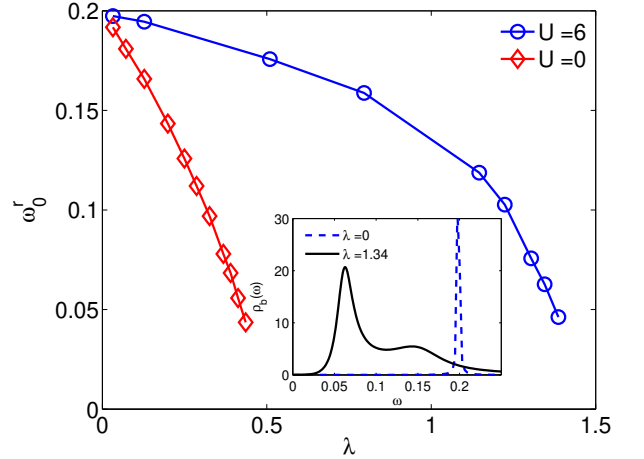


FIG. 3: (Color online) PM calculation: The renormalized phonon frequency ω_0^r as a function of λ for $U = 0$ and $U = 6$. The inset shows the phonon spectral function $\rho_b(\omega)$ for $U = 6$ and $\lambda = 0$ and $\lambda = 1.34$.

A comparison for $1 + \lambda$ with the DMFT results for a series of values can be found in Fig. 2 (d). There are quantitative deviation already at relatively small values of λ and very notable ones for larger λ .¹⁷ Hence, for negligible U a very large kink is obtained already for values of the order $\lambda \sim 0.4$. For larger values of λ a bipolaronic instability occurs where local pairs are formed. At half filling above a critical coupling stable solutions of a bipolaronic insulator can be found as in previous DMFT calculations.^{16,17,20,41} However, in the doped system the calculations become unstable, and results oscillate between solutions with small and large double occupancy.

Paramagnetic DMFT calculations can not provide a suitable ground state solution in these situations.

B. Results for finite U

We now turn to the situation with finite Coulomb repulsion, where we have contributions to $\Sigma(\omega)$ from both interaction terms. Therefore, already for $\lambda = 0$ electrons are renormalized due to scattering processes, which leads to an effective mass enhancement and finite lifetime. For small values of the Coulomb interaction, $U \leq D$, qualitatively similar results to the ones discussed for $U = 0$ can be found for the dispersion relation and the occurrence of kinks.

For larger values of U the situation changes. One important thing to consider is that we have Holstein phonons, i.e. lattice vibrations which couple to *local* fluctuations of the electronic density. Such phonon modes are in direct competition with the Hubbard repulsion, which does exactly the opposite: it tries to freeze density fluctuations out. As a consequence, larger values of λ (compared to $U = 0$) are necessary for observing effects on the dispersion. Furthermore, for values of U relevant for strongly correlated materials, $U \geq W$, the high energy slope does not revert to the non-interacting one for $\varepsilon_{\mathbf{k}} \in (-D, D)$. Thus, when characterizing the kink it does not make sense to compare with the non-interacting slope. Instead one can compare the high and low energy slope within one calculation.

In order to be in a parameter regime roughly suitable for cuprate physics, we choose $n=0.9$ (10% hole doping) and $U=6 > U_{c2}$, $U_{c2} \simeq 5.88$ being the critical value for the metal-insulator transition at half-filling ($n=1$).⁴² We first report the local electronic spectral function for $\lambda = 0$ and $\lambda = 0.86$ in Fig. 4. The well-known three-peak structure can clearly be distinguished, with lower and upper Hubbard bands and a quasiparticle band at the Fermi level $\omega=0$. The spectrum is not symmetric because of the finite hole doping.

One can observe in Fig. 4 that the central quasiparticle peak is relatively little affected by the presence of the electron-phonon coupling. In fact, the effect of the electron-phonon interaction on the low-energy quasiparticle appear just as a small “de-renormalization”; in other words a *decrease* in the effective mass m^* (see Fig. 5d for small values of λ). This result has been already observed at half-filling within DMFT using Lanczos as impurity solver²¹. It can be understood from the physics of the effective impurity model and the Kondo effect connected with the quasiparticle peak. It comes from the fact that the electron-phonon interaction effectively reduces the bare repulsion of the system, making the Kondo coupling somewhat larger. Such a physical mechanism can also be described within perturbation theory, assuming that the scale U associated to the separation between the Kondo peak and the Hubbard bands is the largest, compared to t and ω_0 ⁴³. It is remarkable that we observe this

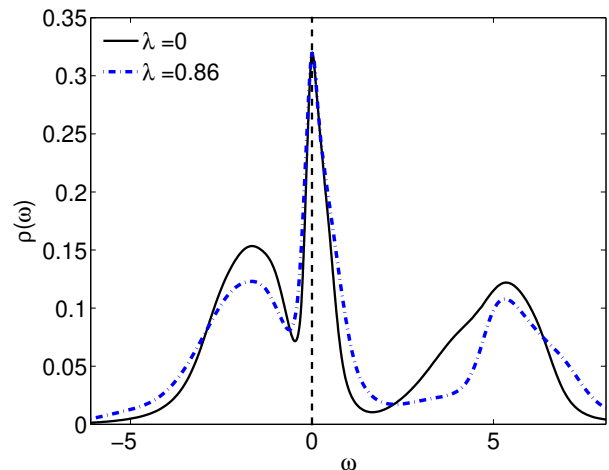


FIG. 4: (Color online) PM calculation: The local electronic spectral function for $U = 6$ and $n = 0.9$.

de-renormalization effect so clearly even away from half-filling, i.e. where the abovementioned separation of energy scales is no longer clearcut (at least for the removal part of the spectrum). Moreover this result convincingly shows how this kind of “protection” of the low-frequency part of the spectrum from phonon effects characteristic of the paramagnetic DMFT solution is present also within the NRG solution. At higher energies instead, one can see differences between the solution with and without λ . Here, contrary to the low-frequency regime, the resolution of our NRG calculation is not accurate enough to resolve the details of the spectra, because of the conventional high-energy broadening used.

Let us now turn to the discussion of the dispersion kink. In Fig. 5 we show a collection of results for the situation with the same U and n and different values of λ . The low energy part of $\rho_{\mathbf{k}}(\omega)$ for $\lambda=0.86$ is shown in Fig. 5 (a) and the corresponding dispersion relation in panel (b).

Comparing the result for $\lambda=0$ and $\lambda=0.86$, we can see how the whole behavior is modified due to the electron-phonon coupling even though no clear kink is visible. We just get a continuous change of the slope for relatively large values of the coupling. We can understand this in light of the arguments given above: the Holstein electron-phonon interaction can not easily induce charge fluctuations due to the direct competition with the Hubbard U . Even though the finite doping reduces the influence of the Mott physics compared to half-filling^{20,44}, the whole low-energy (Kondo-like) physics is still dominated by the electron-electron interaction and room for nontrivial electron-phonon effects is left only for higher-frequency (atomic-like) processes. This has two very important consequences: (i) the low-frequency slope of the dispersion is not strongly affected by the bare electron-phonon coupling and (ii) the deviation between the dispersion with and without phonons (either in the form of a sharp kink or as a smooth change of slope) becomes

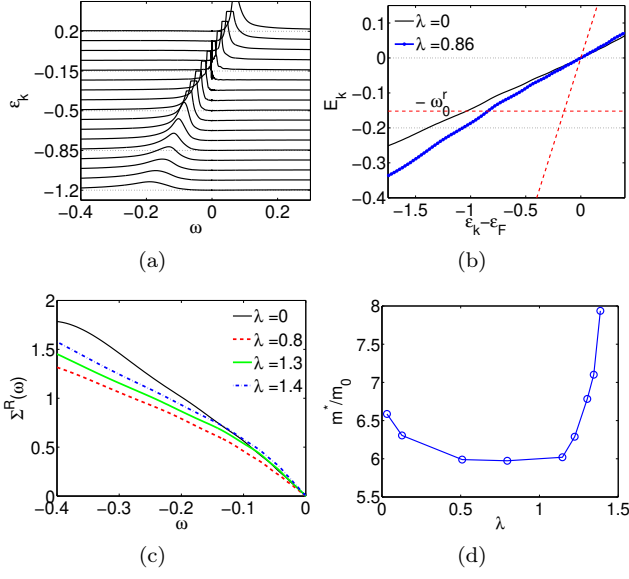


FIG. 5: (Color online) PM calculation: (a) The ε_k resolved spectral function for $U = 6$, $n = 0.9$ and $\lambda = 0.86$. Note that for better visibility of all the peaks, the largest ones have been cut off at a certain value. This generates a small artificial plateau, otherwise absent. (b) The dispersion relation E_k as a function of ε_k for $U = 6$ and $\lambda = 0$ and $\lambda = 0.86$. The horizontal dotted (dashed) line gives the energy ω_0 (ω_0^r), and the dashed line is for free electrons, $E_k = \varepsilon_k$. (c) The real part of the self-energy $\Sigma^R(\omega)$ (with $\Sigma^R(0)$ subtracted) as a function of ω for $U = 6$ and various values of λ . (d) The effective mass as a function of λ .

a *high-frequency electronic* property, in striking contrast with the standard uncorrelated electron-phonon picture in which this is bound to the (renormalized) phonon frequency.

The ω -dependence of the real part of the self-energy, shown in panel (c), consequently shows relatively little modification at low energy and visible one at higher energy. The behavior of the low energy slope and correspondingly effective mass is shown in part (d) as function of λ . As we noted above, there is an initial derrenormalization tendency upon increasing λ , followed by a strong increase of m^* for larger values of λ .

We noted for Fig. 5 (b) that no kink feature can easily be identified. This changes when we increase λ . In Fig. 6 we show the dispersion at a larger value $\lambda=1.34$.

A kink feature is visible at $\omega_k \approx 0.15$ while the renormalized phonon frequency $\omega_0^r \approx 0.063$ (extracted from the maximum of the phonon spectral function $\rho_b(\omega)$ see inset Fig. 3). This clearly shows how these two quantities, always bound to go hand in hand in a conventional uncorrelated metal as two aspects of the same physical phenomenon, can instead be different in a system which is described within paramagnetic DMFT. The renormalized phonon frequency ω_0^r still describes the influence of electron-phonon coupling on the phonon spectral function, while the kink position ω_k is associated to the en-

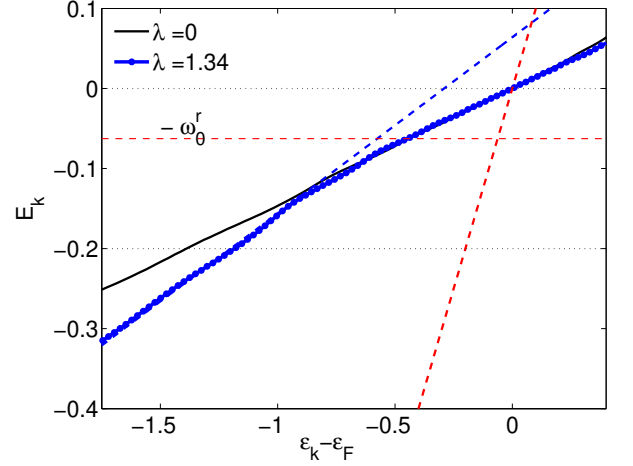


FIG. 6: (Color online) PM calculation: The dispersion relation E_k as a function of ε_k for $U = 6$, $n = 0.9$ and different values of electron-phonon coupling. Included is a dashed line to fit the high energy slope of the dispersion.

ergy range in the electronic spectrum where phonon effects become visible. The latter is a new energy scale of the problem, which comes out of the competition between the instantaneous Hubbard repulsion and the retarded phonon-mediated attraction. It is interesting to see that, as seen in the inset of Fig. 3, $\rho_b(\omega)$, which for $\lambda = 0$ is a delta function peaked at ω_0 , possesses a considerable amount of spectral weight for energies larger than ω_0^r for this situation. By numerical fitting the magnitude of the kink was extracted to be $m_k \approx 1.55$. When we increase λ further to overcome U , strong polaronic behavior will eventually dominate the low energy behavior again.

Another possibility to find a kink due to electron-phonon coupling in the presence of large U is to increase the doping, as the effect of U to freeze the charge fluctuations is weakened then. We give an example for $\lambda = 0.86$ and 20% doping in Fig. 7.

A weak kink feature can be identified at higher energy. This is more pronounced in calculations for larger values of λ , but we stick to this value for comparison to later results. The magnitude of the kink is by numerical fitting $m_k \approx 1.39$. Notice that also here the kink position is larger than the renormalized phonon energy. When we further increase the doping m_k will become larger and ω_k will, for $n \sim 0.5$, eventually coincide²² with ω_0^r as expected in the conventional picture.

We cannot compare the DMFT results obtained so far to experiments on cuprates as we have not yet introduced any effect coming from antiferromagnetic correlations. These are known to play a crucial role for small doping values, therefore we have to include them in our model calculation. One way of doing this is to let the system have long-range order so that we can describe (a classical mean-field version of) the physics of antiferromagnetic exchange. This is what is done in the following section.

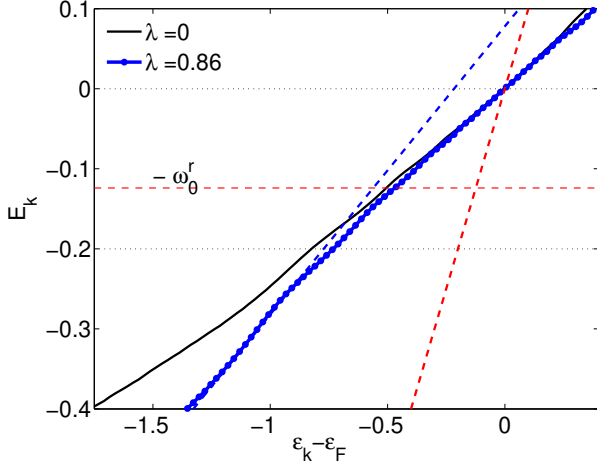


FIG. 7: (Color online) PM calculation: The dispersion relation $E_{\mathbf{k}}$ as a function of $\varepsilon_{\mathbf{k}}$ for $U = 6$, $n = 0.8$ and different values of electron-phonon coupling. Included is a dashed line to fit the high energy slope of the dispersion.

III. KINKS AND ANTIFERROMAGNETIC CORRELATIONS

In order to include antiferromagnetic correlations we assume a bipartite lattice with A and B sublattice and, as in the standard DMFT implementation for long-range ordered phases^{18,35–37}, we write the matrix Green's function in the form

$$\underline{G}_{\mathbf{k},\sigma}(\omega) = \frac{1}{\zeta_{A,\sigma}(\omega)\zeta_{B,\sigma}(\omega) - \varepsilon_{\mathbf{k}}^2} \begin{pmatrix} \zeta_{B,\sigma}(\omega) & \varepsilon_{\mathbf{k}} \\ \varepsilon_{\mathbf{k}} & \zeta_{A,\sigma}(\omega) \end{pmatrix}, \quad (4)$$

with $\zeta_{\alpha,\sigma}(\omega) = \omega + \mu_{\alpha,\sigma} - \Sigma_{\alpha,\sigma}(\omega)$, $\alpha = A, B$. For the AF order one has $\mu_{A,\sigma} = \mu - \sigma h_s$, $\mu_{B,\sigma} = \mu + \sigma h_s$, and the condition $\Sigma_{B,\sigma}(\omega) = \Sigma_{A,-\sigma}(\omega)$. We consider solutions where the symmetry breaking field vanishes, $h_s \rightarrow 0$. As we do not have any next-nearest neighbor hopping, the antiferromagnetic solution is lower in energy than the paramagnetic one for small values of the doping³⁵.

The form of the dispersion as found from the poles of the Green's function in Eq. (4) can be obtained from the equation

$$\omega_{\pm} = -\bar{\mu} + \Sigma^+(\omega) \pm \sqrt{(\Delta\bar{\mu} - \Sigma^-(\omega))^2 + \varepsilon_{\mathbf{k}}^2}, \quad (5)$$

where we only included the real parts of the self-energies. We defined $\bar{\mu} = (\bar{\mu}_{\uparrow} + \bar{\mu}_{\downarrow})/2$, $\Delta\bar{\mu} = (\bar{\mu}_{\uparrow} - \bar{\mu}_{\downarrow})/2$ with $\bar{\mu}_{\sigma} = \mu_{\sigma} - \Sigma_{\sigma,0}$, and we have split into static and dynamic part in the self-energy, $\text{Re}\Sigma_{\sigma}(\omega) = \Sigma_{\sigma,0} + \bar{\Sigma}_{\sigma}(\omega)$. We also introduced $\Sigma^{\pm}(\omega) = (\bar{\Sigma}_{\uparrow}(\omega) \pm \bar{\Sigma}_{\downarrow}(\omega))/2$. The solution of Eq. (5) as an implicit equation gives the dispersion $E_{\mathbf{k},\pm}$ in the AF case. The mean field solution without phonons gives the two Slater bands, and upon hole doping the Fermi level moves into the lower one. By making a simple ansatz for the electron-phonon part of the self-energy, $\bar{\Sigma}_{\sigma}^g(\omega) = -\lambda_{\sigma}\omega\theta(\omega_0 - |\omega|)$ with $\lambda = (\lambda_{\uparrow} + \lambda_{\downarrow})/2$, one

can show that the different form of the equation does not lead to the occurrence of larger kinks in the dispersion relation than in the PM case, Eq. (3).

Several studies pointed out the importance of cooperative effects between lattice- and spin-polarons^{37,45}, influencing both photoemission^{28,29,46–50} and optical properties^{51–53} of correlated systems. By studying antiferromagnetism in the Hubbard-Holstein model within DMFT it was clarified that a finite doping weakens these cooperative effects²³. However, the values of λ at which polarons are obtained in the antiferromagnetic phase are not only much smaller than the values needed to form local bipolarons but are also smaller than those needed to observe polaronic features in paramagnetic DMFT spectra²³. It is interesting to note that Dynamical Cluster Approximation (DCA) calculations²⁴ confirmed the picture found in AF-DMFT, even though short-range AF correlations in DCA are realistically present already at the paramagnetic level.

The present AF-DMFT NRG study has the big advantage that we can resolve low-energy features in the spectral function at finite doping in a way that is beyond any of the previous exact diagonalization and Monte Carlo studies. In Fig. 8 we show the spin-resolved local spectral function in AF-DMFT solved with NRG. The parameters, $U=6$ and $n=0.9$, are the same as in Fig. 4 and 5(b) where the spectral function without antiferromagnetic correlations was shown. As one can see the Fermi energy has moved into the lower band and at low energy the typical square root divergence in $\rho_{\uparrow}(\omega)$ appears. At the same time the minority spin $\rho_{\downarrow}(\omega)$ displays the square root decrease. Hubbard band features at higher energies can also be identified.

The sublattice spectral functions of the AF solution at 10% doping and $U = 6$ show qualitatively similar features for $\lambda = 0$ and $\lambda = 0.86$ as seen in Fig. 8. The spectrum at $\lambda=0.86$ displays a strong quasiparticle excitation at the gap edge, with no big sign of renormalization. Yet the effect of the electron-phonon interaction is still much stronger than in the paramagnetic DMFT at the same U . To see this we show in Fig. 9 the dispersion relation for the same set of parameters, comparing again $\lambda=0$ with $\lambda=0.86$.

A kink in $E_{\mathbf{k}}$ is visible, while (see Fig. 5b) just a smooth change in the slope could be observed for the same value of λ without the AF correlations. By numerical fitting we can extract a magnitude of the kink of $m_{\mathbf{k}} \approx 1.64$. When doping is decreased or λ increased the kink becomes even more pronounced. Similar values of $m_{\mathbf{k}}$ within the paramagnetic phase are reached only taking $\lambda=1.34$. Therefore, the qualitative difference between paramagnetic and AF-DMFT coming from the underlying spin background reflects in a big quantitative difference in the strength of the kink. This is expected from the above arguments, but has not been shown explicitly for the dispersion relation.

Particularly interesting for the present study is the kink position $\omega_{\mathbf{k}}$ in AF-DMFT. Contrary to the paramagnetic phase studied in Sec. II B, the kink in the elec-

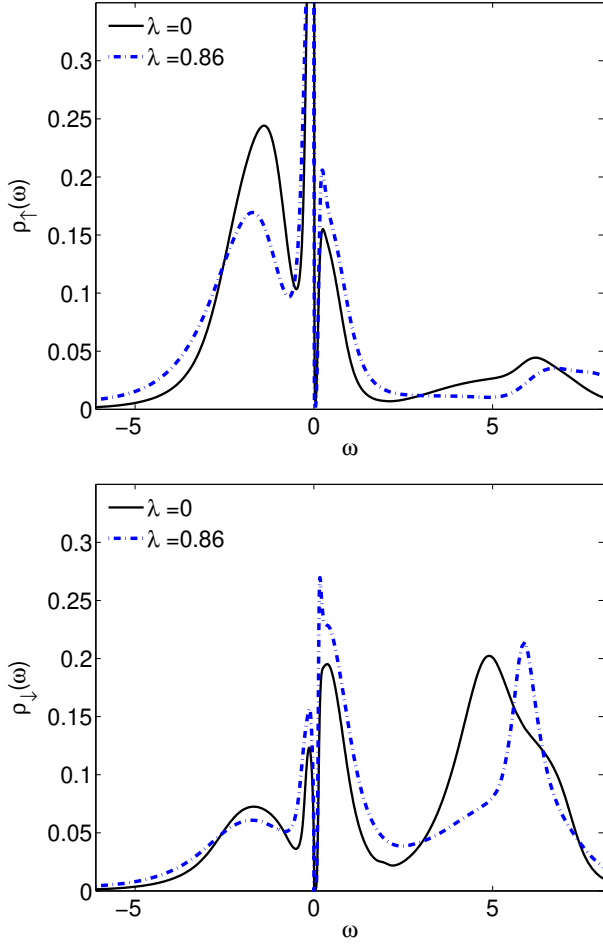


FIG. 8: (Color online) AF calculation: The local electronic spectral density for majority electrons $\rho_{\uparrow}(\omega)$ and minority electrons $\rho_{\downarrow}(\omega)$.

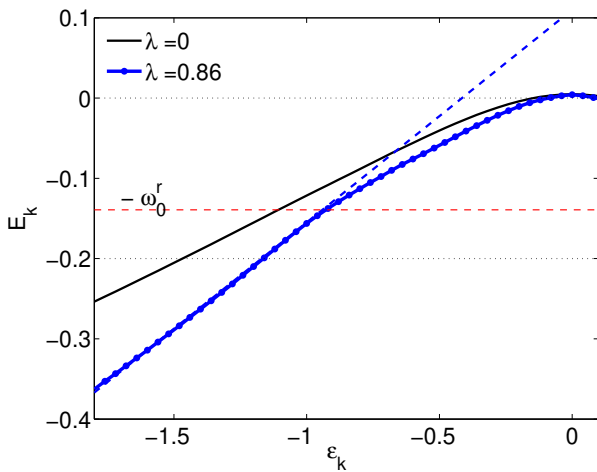


FIG. 9: (Color online) AF calculation: The dispersion relation $E_{\mathbf{k}}$ as a function of $\varepsilon_{\mathbf{k}}$ for $U = 6$, $n = 0.9$ and different values of electron-phonon coupling. Included is a dashed line to fit the high energy slope of the dispersion.

tronic dispersion is *at* (or even slightly before) the renormalised frequency $\omega_0^r \simeq 0.16$, as shown in Fig. 9. This is very different from the paramagnetic DMFT result of the previous section, for which ω_k loses its connection with the renormalized phonon frequency and becomes a higher frequency electronic property. For the values of λ or doping range where a clear kink can be identified ($\lambda = 1.34$, $n \leq 0.8$), indeed, paramagnetic DMFT gives a renormalized phonon frequency $\omega_0^r < \omega_k$. Therefore we conclude that paramagnetic and antiferromagnetic DMFT calculations can differ qualitatively in the physics behind the kink: in paramagnetic DMFT a larger λ or larger doping is needed to form a kink and the kink energy is not pinned to the renormalized phonon frequency, but rather is connected to a higher energy scale at the crossover between the Kondo-like physics and a more atomic-like one. In AF-DMFT a smaller value of λ is enough to see a kink and the position of this kink closely tracks the renormalized phonon frequency.

The stronger electron-phonon effects on the AF electronic dispersion are connected directly to the real part of the self-energy, shown in Fig. 10 for the majority (\uparrow) and minority (\downarrow) spin component on the sublattice. Without the electron-phonon coupling minority electrons scatter much stronger with the majority spin electrons and therefore the slope of $\Sigma_{\downarrow}^R(\omega)$ is larger than the one of $\Sigma_{\uparrow}^R(\omega)$ for $\lambda = 0$.³⁶ When λ is increased, we can see that the low energy slope changes relatively little for $\Sigma_{\uparrow}^R(\omega)$. At $\lambda \geq 0.86$ a feature at $\omega \simeq \omega_0^r$ can be identified in $\Sigma_{\uparrow}^R(\omega)$, which gives rise to the kink in the dispersion in Fig. 9. In calculations for larger λ , smaller doping or smaller U this is more pronounced. This is related to the cooperative effect of the magnetic polaron interacting with phonons which was discussed earlier. The low energy slope of $\Sigma_{\downarrow}^R(\omega)$ decreases on increasing λ and no clear feature is seen around $\omega \simeq \omega_0^r$.

For small values of U and λ these results for the self-energies can be understood from a perturbative calculation to order g^2 (see Fig. 1). As a starting point one can use the doped AF state and calculate the lowest order self-energy corrections due to coupling to the phonons. Then it is found that the majority spin electrons scatter much stronger with the phonons as the minority ones, and are therefore much stronger renormalized. $\Sigma_{\uparrow}^R(\omega)$ shows a much more pronounced logarithmic divergence at ω_0^r than in the normal state discussed in Sec. II. Formally, this comes from the enhanced density of states at the Fermi level which is a consequence of the AF order. An intuitive understanding can be motivated by considering that majority spin electrons on a sublattice are surrounded on average by the opposite spin direction. This provides an energetic gain, but also leads to some degree of localization, as an itinerant excitation destroys the antiferromagnetic order. This effect can cooperate with the coupling to the phonons inducing a further renormalization and as a result majority spins are more affected than without the ordered background. At the same time minority spin electrons couple less to the

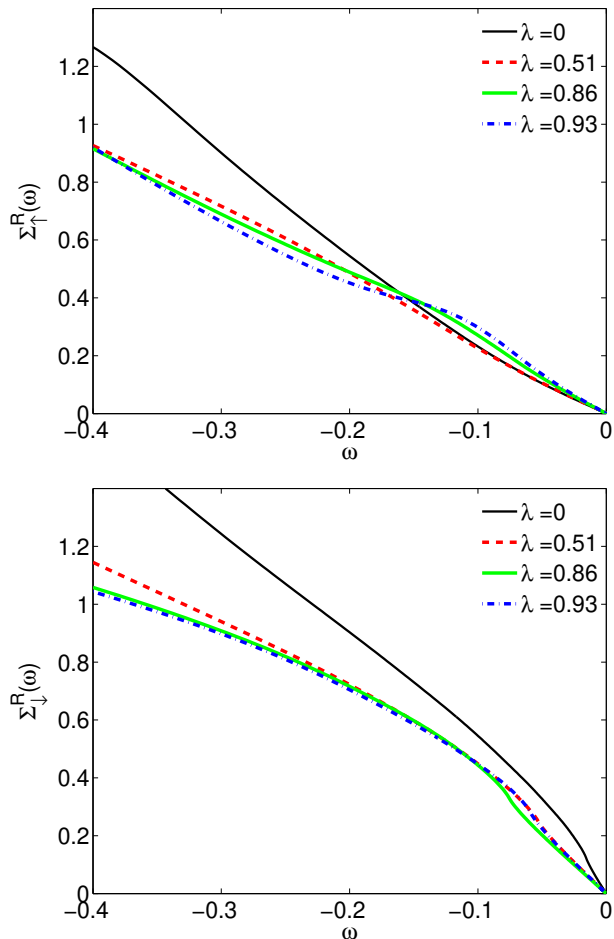


FIG. 10: (Color online) AF calculation: The real part of the selfenergies $\Sigma_{\uparrow}^R(\omega)$ (upper panel) and $\Sigma_{\downarrow}^R(\omega)$ (lower panel) with $\Sigma_{\sigma}^R(0)$ subtracted.

phonons. In addition to the different renormalization effects, the electron-phonon coupling can lead to a stabilisation and even an increase of the magnetization. These weak coupling considerations qualitatively carry over to the stronger coupling case relevant for the results above. However, additional renormalization effects due to U play a role then and make a perturbative treatment difficult.

IV. CONCLUSIONS

We have described the occurrence of kinks in the electronic dispersion relation due to coupling to a local phonon mode taking into account strong electronic correlations. As anticipated our results show that the simple theory of kinks is modified for both strong electron-phonon and electron-electron coupling. For the paramagnetic state and small doping from half filling a clear kink is not visible anymore for large values of $U > W$ unless the electron-phonon coupling assumes large values. The phonons can have an effect at higher energy whilst the

low energy features are less affected. An important finding is that the effect of U to suppress the occurrence of kinks is less efficient if we allow for antiferromagnetic correlations. Then a cooperative effect leads to a stronger effective coupling of the electronic quasiparticles (magnetic polarons) to the phonons. That something like this can happen has been observed in earlier studies^{23,54}. Here we clarify how this manifests itself for kinks. Nevertheless for the type of phonons we study in competition with the Coulomb interaction we find that inspite of relatively large values, $\lambda \simeq 0.8$, kink features are moderate even with antiferromagnetic correlations, $m_k \simeq 1.6$. This may be a consequence of the type of phonons we study (Holstein). Some works have indeed shown that non-Holstein phonons have stronger polaronic effects in correlated systems, due to a less direct competition with the local Hubbard repulsion^{55–57}. Therefore a quantitative comparison with results for the low-energy kink in cuprate superconductors, or a statement about the origin of the nodal kink in these systems is hard to make here.

Still, we can relate our findings to the puzzling results for the kink position reported by Kordyuk *et al.* in Ref. 13. There, as already discussed in the Introduction, a suprisingly strong dependence on doping and temperature of the kink position was observed. Nothing like this is can be obtained within conventional electron-phonon theories. Our results show that, by taking the effect of electronic correlation properly into account, the kink position becomes strongly dependent on the strength of antiferromagnetic correlations. We found that when AF correlations are strong, the kink is close to the renormalized phonon frequency (i.e. is more “low energy”), while when AF correlations are absent, the kink can occur at higher frequencies and also needs a larger electron-phonon coupling to be of similar strength. Therefore it is very plausible to expect that, at low doping, where AF correlations are stronger, the kink energy is small in absolute value (see Fig. 9), while at larger values of the doping, where AF correlations are weaker, the kink occurs at larger energies (see Fig. 7). Interestingly, this is exactly the trend shown in the data on the Bi-compound at the lowest temperature¹³.

Generally, it is very important to test - as we do here - the predictions of theories which, like paramagnetic and AF-DMFT, describe electron-phonon *and* strong electronic correlations on an equal footing. Strong coupling to a phonon mode is very often discarded as being responsible for the nodal kink in cuprates on the basis of clichés coming from conventional theories neglecting electronic correlations. The doping dependence is one typical example. Our study shows instead that, when including correlation, properties like the doping dependence of the kink energy may become highly non-trivial, and therefore the conventional picture cannot be used to rule out phonons.

Acknowledgment

We wish to thank O. Gunnarsson, A.C. Hewson and D.

Manske for useful discussions and O. Gunnarsson for critically reading of the manuscript. G.S. acknowledges fi-

nancial support from the FWF 'Lise-Meitner' Grant No. M1136.

- ¹ A. Lanzara, P. V. Bogdanov, X. J. Zhou, S. A. Keller, D. L. Feng, E. D. Lu, T. Yoshida, H. Eisaki, A. Fujimori, K. Kishio, et al., *Nature* **412**, 510 (2001).
- ² J. Graf, M. d'Astuto, C. Jozwiak, D. R. Garcia, N. L. Saini, M. Krisch, K. Ikeuchi, A. Q. R. Baron, H. Eisaki, and A. Lanzara, *Phys. Rev. Lett.* **100**, 227002 (2008).
- ³ L. Pintschovius and W. Reichardt, in *Neutron Scattering in Layered Copper-Oxide Superconductors*, edited by A. Furrer (Kluwer Academic, Dordrecht, 1998), vol. 20, p. 165.
- ⁴ H. Iwasawa, J. F. Douglas, K. Sato, T. Masui, Y. Yoshida, Z. Sun, H. Eisaki, H. Bando, A. Ino, M. Arita, et al., *Phys. Rev. Lett.* **101**, 157005 (2008).
- ⁵ T. Dahm, V. Hinkov, S. V. Borisenko, A. A. Kordyuk, V. B. Zabolotnyy, J. Fink, B. Büchner, D. J. Scalapino, W. Hanke, and B. Keimer, *Nature Phys.* **5**, 217 (2009).
- ⁶ P. D. Johnson, T. Valla, A. V. Fedorov, Z. Yusof, B. O. Wells, Q. Li, A. R. Moodenbaugh, G. D. Gu, N. Koshizuka, C. Kendziora, et al., *Phys. Rev. Lett.* **87**, 177007 (2001).
- ⁷ D. Manske, I. Eremin, and K. H. Bennemann, *Phys. Rev. Lett.* **87**, 177005 (2001).
- ⁸ A. V. Chubukov and M. R. Norman, *Phys. Rev. B* **70**, 174505 (2004).
- ⁹ M. Eschrig, *Adv. Phys.* **55**, 47 (2006).
- ¹⁰ D. Reznik, G. Sangiovanni, O. Gunnarsson, and T. P. Devereaux, *Nature* **455**, E6 (2008).
- ¹¹ A. S. Mishchenko, *Phys. Usp.* **52**, 1193 (2009).
- ¹² X. J. Zhou, T. Yoshida, A. Lanzara, P. V. Bogdanov, S. A. Kellar, K. M. Shen, W. L. Yang, F. Ronning, T. Sasagawa, T. Kakeshita, et al., *Nature* **423**, 398 (2003).
- ¹³ A. A. Kordyuk, S. V. Borisenko, V. B. Zabolotnyy, J. Geck, M. Knupfer, J. Fink, B. Büchner, C. T. Lin, B. Keimer, H. Berger, et al., *Phys. Rev. Lett.* **97**, 017002 (2006).
- ¹⁴ S. Engelsberg and J. R. Schrieffer, *Phys. Rev.* **131**, 993 (1963).
- ¹⁵ P. Benedetti and R. Zeyher, *Phys. Rev. B* **58**, 14320 (1998).
- ¹⁶ D. Meyer, A. Hewson, and R. Bulla, *Phys. Rev. Lett.* **89**, 196401 (2002).
- ¹⁷ M. Capone and S. Ciuchi, *Phys. Rev. Lett.* **91**, 186405 (2003).
- ¹⁸ A. Georges, G. Kotliar, W. Krauth, and M. Rozenberg, *Rev. Mod. Phys.* **68**, 13 (1996).
- ¹⁹ T. Maier, M. Jarrell, T. Pruschke, and M. H. Hettler, *Rev. Mod. Phys.* **77**, 1027 (2005).
- ²⁰ W. Koller, D. Meyer, and A. C. Hewson, *Phys. Rev. B* **70**, 155103 (2004).
- ²¹ G. Sangiovanni, M. Capone, C. Castellani, and M. Grilli, *Phys. Rev. Lett.* **94**, 026401 (2005).
- ²² W. Koller, A. C. Hewson, and D. M. Edwards, *Phys. Rev. Lett.* **95**, 256401 (2005).
- ²³ G. Sangiovanni, O. Gunnarsson, E. Koch, C. Castellani, and M. Capone, *Phys. Rev. Lett.* **97**, 046404 (2006).
- ²⁴ A. Macridin, B. Moritz, M. Jarrell, and T. Maier, *Phys. Rev. Lett.* **97**, 056402 (2006).
- ²⁵ P. Werner and A. J. Millis, *Phys. Rev. Lett.* **99**, 146404 (2007).
- ²⁶ J. Bauer, *Europhys. Lett.* **90**, 27002 (2010).
- ²⁷ J. Bauer and A. C. Hewson, *Phys. Rev. B* **81**, 235113 (2010).
- ²⁸ A. S. Mishchenko and N. Nagaosa, *Phys. Rev. Lett.* **93**, 036402 (2004).
- ²⁹ O. Rösch and O. Gunnarsson, *Phys. Rev. Lett.* **93**, 237001 (2004).
- ³⁰ O. Rösch and O. Gunnarsson, *Phys. Rev. B* **70**, 224518 (2004).
- ³¹ K. Wilson, *Rev. Mod. Phys.* **47**, 773 (1975).
- ³² R. Bulla, T. Costi, and T. Pruschke, *Rev. Mod. Phys.* **80**, 395 (2008).
- ³³ R. Peters, T. Pruschke, and F. B. Anders, *Phys. Rev. B* **74**, 245114 (2006).
- ³⁴ A. Weichselbaum and J. von Delft, *Phys. Rev. Lett.* **99**, 076402 (2007).
- ³⁵ R. Zitzler, T. Pruschke, and R. Bulla, *Eur. Phys. J. B* **27**, 473 (2002).
- ³⁶ J. Bauer and A. C. Hewson, *Eur. Phys. J. B* **57**, 235 (2007).
- ³⁷ G. Sangiovanni, A. Toschi, E. Koch, K. Held, M. Capone, C. Castellani, O. Gunnarsson, S. Mo, J. W. Allen, H. Kim, et al., *Phys. Rev. B* **73**, 205121 (2006).
- ³⁸ T. Cuk, D. H. Lu, X. J. Zhou, Z.-X. Shen, T. P. Devereaux, and N. Nagaosa, *phys. stat. sol. (b)* **242**, 11 (2005).
- ³⁹ O. Gunnarsson and O. Rösch, *J. Phys.: Condens. Matter* **20**, 043201 (2008).
- ⁴⁰ W. Metzner and D. Vollhardt, *Phys. Rev. Lett.* **62**, 324 (1989).
- ⁴¹ G. Sangiovanni, C. Castellani, and M. Capone, *Phys. Rev. B* **73**, 165123 (2006).
- ⁴² R. Bulla, *Phys. Rev. Lett.* **83**, 136 (1999).
- ⁴³ P. S. Cornaglia, H. Ness, and D. R. Grempel, *Phys. Rev. Lett.* **93**, 147201 (2004).
- ⁴⁴ G. Sangiovanni, M. Capone, C. Castellani, and M. Grilli, *Phys. Rev. Lett.* **94**, 026401 (2005).
- ⁴⁵ R. Strack and D. Vollhardt, *Phys. Rev. B* **46**, 13852 (1992).
- ⁴⁶ G. Wellein, H. Röder, and H. Fehske, *Phys. Rev. B* **53**, 9666 (1996).
- ⁴⁷ E. Cappelluti and S. Ciuchi, *Phys. Rev. B* **66**, 165102 (2002).
- ⁴⁸ V. Cataudella, G. De Filippis, A. S. Mishchenko, and N. Nagaosa, *Phys. Rev. Lett.* **99**, 226402 (2007).
- ⁴⁹ O. Gunnarsson and O. Rösch, *Phys. Rev. B* **73**, 174521 (2006).
- ⁵⁰ S. Kar and E. Manousakis, *Phys. Rev. B* **78**, 064508 (2008).
- ⁵¹ B. Bäuml, G. Wellein, and H. Fehske, *Phys. Rev. B* **58**, 3663 (1998).
- ⁵² A. S. Mishchenko, N. Nagaosa, Z.-X. Shen, G. De Filippis, V. Cataudella, T. P. Devereaux, C. Bernhard, K. W. Kim, and J. Zaanen, *Phys. Rev. Lett.* **100**, 166401 (2008).
- ⁵³ E. Cappelluti, S. Ciuchi, and S. Fratini, *Phys. Rev. B* **79**, 012502 (2009).
- ⁵⁴ A. Macridin, B. Moritz, M. Jarrell, and T. Maier, *Phys. Rev. Lett.* **97**, 056402 (2006).
- ⁵⁵ O. Rösch and O. Gunnarsson, *Phys. Rev. Lett.* **92**, 146403 (2004).
- ⁵⁶ G. D. Filippis, V. Cataudella, R. Citro, C. A. Peroni, A. S. Mishchenko, and N. Nagaosa (2010),

<http://arxiv.org/abs/1004.2815>.

- ⁵⁷ S. Johnston, F. Vernay, B. Moritz, Z.-X. Shen, N. Nagaosa, J. Zaanen, and T. P. Devereaux, Phys. Rev. B **82**, 064513 (2010).